

Article

Not peer-reviewed version

Polydopamine-Coated Polycaprolactone Electrospun Nanofiber Membrane Loaded with Thrombin for Wound Hemostasis

Dapeng Cui [†], [Ming Li](#) [†], Peng Zhang, Feng Rao, [Wei Huang](#), Chuanlin Wang, [Wei Guo](#) ^{*}, [Tianbing Wang](#) ^{*}

Posted Date: 25 June 2023

doi: 10.20944/preprints202306.1698.v1

Keywords: Trauma; Electrospinning technology; Polydopamine modification; Thrombin; Hemostatic method



Preprints.org is a free multidiscipline platform providing preprint service that is dedicated to making early versions of research outputs permanently available and citable. Preprints posted at Preprints.org appear in Web of Science, Crossref, Google Scholar, Scilit, Europe PMC.

Copyright: This is an open access article distributed under the Creative Commons Attribution License which permits unrestricted use, distribution, and reproduction in any medium, provided the original work is properly cited.

Article

Polydopamine-Coated Polycaprolactone Electrospun Nanofiber Membrane Loaded with Thrombin for Wound Hemostasis

Dapeng Cui ^{1,†}, Ming Li ^{2,3,4,†}, Peng Zhang ^{2,3,4}, Feng Rao ^{2,3,4}, Wei Huang ^{2,3,4}, Chuanlin Wang ^{2,3,4}, Wei Guo ^{2,3,4,*} and Tianbing Wang ^{2,3,4,*}

¹ Hepatobiliary Surgery Department, the First Affiliated Hospital of Hebei North University, Zhangjiakou, Hebei, 075000

² Trauma Medicine Center, Peking University People's Hospital, Beijing, 100044, China

³ Key Laboratory of Trauma and Neural Regeneration, Peking University, Ministry of Education, Beijing, 100044, China

⁴ National Center for Trauma Medicine, Beijing, 100044, China

* Correspondence: woaiguowei111@sina.com (Wei Guo); wangtianbing@pkuph.edu.cn (Tianbing Wang)

† Dapeng Cui and Ming Li contributed equally to this work.

Abstract: Hemorrhagic shock is the primary cause of death in patients with severe trauma, and the development of rapid and efficient hemostatic methods is of great significance in promoting the life-saving of trauma patients. In this study, polycaprolactone (PCL) nanofiber membrane was prepared by electrospinning technology. The PCL-PDA loading system was developed by modifying the surface of polydopamine (PDA) inspired by mussel adhesion protein, and the efficient and stable loading of thrombin (TB) was realized on the premise of ensuring the bioactivity of TB. The new thrombin loading system overcomes the disadvantages of harsh storage conditions, poor strength, easy to fall off, and can use thrombin to start rapid coagulation cascade reaction, which has the characteristics of fast hemostasis, good biocompatibility, high safety and wide range of hemostasis. The physicochemical properties and biocompatibility of PCL-PDA-TB membrane were verified by scanning electron microscopy, cell proliferation test, cell adhesion test and extract cytotoxicity test. Red blood cell adhesion, platelet adhesion, dynamic coagulation time and animal models all verified the coagulation effect of PCL-PD-TB membrane. Therefore, PCL-PDA-TB membrane has great potential in wound hemostasis.

Keywords: trauma; electrospinning technology; polydopamine modification; thrombin; hemostatic method

1. Introduction

In the emergency department, trauma-induced hemorrhagic shock is the leading cause of death [1–3]. Therefore, rapid and efficient hemostatic first aid measures are essential to save the lives of trauma patients, especially for traumatic bleeding of the liver, spleen, kidneys and other substantial visceral trauma and bleeding of large vessels such as aorta, femoral artery and mesenteric artery [4–7]. At present, the commonly used hemostatic materials in clinical practice include gelatin sponge, fibrin glue, polysaccharide hemostatic powder, etc. [8–10], whose the main hemostatic mechanisms include: material adsorbs and networks the formation components in the blood, thereby providing a mechanical structure for the mutual adhesion between platelets and promoting thrombosis; material compresses hemostasis by absorbing water and expanding or mechanical hemostasis formed by dissolving the adhesion wound; Hemostatic materials exert hemostatic effects by carrying procoagulant drugs [11–13]. However, these hemostatic materials still have certain limitations, such as low hemostatic efficiency, poor biocompatibility, harsh storage and use conditions, etc., which

cannot fully meet the urgent needs of all trauma first aid [14,15]. Exploring and developing new rapid hemostatic materials with better performance is still an urgent clinical need.

Thrombin is a serine protease extracted from human or animal blood. It is a biological factor that plays a major role in the coagulation cascade, which can activate FXIII and convert fibrinogen in the blood into fibrin to achieve hemostasis [16]. As we all know, thrombin has many advantages: a variety of bleeding wound types, rapid function, reasonable biocompatibility and non-toxic, easy to obtain and use, etc., which is widely used in capillaries, small blood vessels and organs to stop bleeding, and has excellent hemostatic effect [17,18]. But on the other hand, because of its almost non-adhesion, when used for bleeding in larger wounds, it is easy to be washed away by the blood flow and lose its hemostatic effect; and its harsh storage environment (low temperature) further limits its range of applications [19,20]. Therefore, it is important to develop thrombin loaded membranes or other materials instead of powder-based materials.

The thrombin can be linked by a polymer to convert the thrombin powder into a thrombin membrane for acute hemostasis. The nanofiber membrane prepared by electrospinning technology has larger specific surface area, smaller pore size and higher porosity, which can simulate many natural tissues and organs, and is widely used in medical bioengineering fields such as artificial blood vessels, drug delivery carriers and tissue repair [21,22]. PCL is often used as a raw material in electrospinning technology. It is a commonly used biodegradable polymer synthetic material that degrades into non-toxic metabolites in vivo [23–25]. However, due to the hydrophobic surface structure of pure polymer electrospun membrane, it is difficult for proteins and cells to attach, resulting in low drug loading efficiency, poor cell affinity and poor biological activity.

In recent years, polydopamine (PDA) coating, as a simple and mild surface modification method, can improve the adhesion properties of modified biomaterials, and has been widely concerned by researchers. Due to its good biocompatibility and its ability to promote cell proliferation [26], PDA has been used in many fields to develop bioactive molecular delivery systems. For example, PDA coated chitosan membranes are used to deliver vascular endothelial growth factor (VEGF) in vascular tissue engineering [27]. In addition, PCL-nanocarbon fiber scaffolds coated with PDA are used to deliver Brain-derived neurotrophic factor (BDNF) in nerve repair [28]. However, the study of using PDA surface modification to efficiently load thrombin on nanofiber membrane for wound hemostasis has not been reported so far.

To this end, in this study, the PCL nanofiber membrane was prepared by electrospinning method, and thrombin was loaded onto the membrane by PDA surface modification. The loading efficiency was evaluated using TB model protein (FITC-BSA). Then, fibroblasts were co-cultured with membranes to evaluate the effects of membranes on fibroblast growth and adhesion. Further, subcutaneous embedding models of SD rats were used to evaluate the biosafety of the membranes in vivo. Then, the in vitro coagulability of membranes was tested by dynamic coagulation test and adhesion test of red blood cells and platelets. Finally, the in vivo coagulability of membranes was evaluated using SD rat liver hemorrhage model and femoral artery hemorrhage model.

2. Materials and Methods

2.1. Preparation of PCL Fibrous Membranes

1g Polycaprolactone (PCL, Jinan Daigang Co., Ltd., Jinan, China) was added into 10ml chloroform (McLean Reagent Co., Ltd., Beijing, China) and N, N-dimethylformamide (McLean Reagent Co., Ltd., Beijing, China) in a mixed solvent (8:2, v/v), and stirred with a magnetic stirrer until completely dissolved to obtain spinning solution. Load the prepared electrospinning solution into a 20 mL syringe, set the electrospinning voltage to 25 kV, the solution flow rate to 1.0 mL/h, the receiving distance to 16 cm, the temperature to 25 °C, and the humidity to 50%. The PCL fibrous membranes obtained by electrospinning machine was placed in a fume hood for some time to allow the solvent to fully evaporate, and then dried in a vacuum oven for 6 hours to completely remove residual solvent, then a preliminary PCL fibrous membrane was obtained.

2.2. Coating PDA onto PCL Fibrous Membranes

Dopamine (McLean Reagent Co., Ltd., Beijing, China) was dissolved in 10 mM Tris HCl (pH=8.5) to prepare 2 mg/mL dopamine solution. Placed the PCL nanofiber membrane in a dopamine solution, soak it in dark for 12 hours, washed it with deionized water three times, freeze-dried it to obtain the PCL-PDA fibrous membrane.

2.3. Characterization of Membranes

Sprayed gold on PCL and PCL-PDA fibrous membranes, and observed the morphology of the fibrous membranes using field emission scanning electron microscopy (SEM, HITACHI SU8010, Japan). The surface chemical elements of PCL and PCL-PDA fibrous membranes were analyzed by energy-dispersive spectroscopy (EDS) and elemental mapping. Used Image-Pro Plus 6.0 software (Media Cybernetics, Rockville, MD, USA) to analyze the distribution of nanofiber diameter. The water contact angles of the PCL and PCL-PDA fibrous membranes were measured with a water contact angle tester (OCA20, DataPhysics, Filderstadt, Germany).

2.4. Thrombin Loading

Prepared a TB solution with a concentration of 250 U/mL, soaked the PCL and PCL-PDA fibrous membranes in the TB solution for 12 hours, washed it with deionized water three times, freeze-dried to obtain a PCL-TB and PCL-PDA-TB fibrous membranes. The TB loaded on the fiber scaffold was observed by SEM. The surface chemical elements of PCL-PDA-TB fiber membranes were analyzed by energy dispersive spectrometry (EDS) and element diagram.

In order to evaluate the distribution of TB on the membranes, fluorescein isothiocyanate-labeled bovine serum albumin (FITC-BSA) (Solarbio, Beijing, China) was applied as a model drug for TB according to the procedure described above. After FITC-BSA loading, the membranes were harvested, washed with deionized water and observed using a confocal laser scanning microscope (CLSM) (TCS-SP8, Leica, Wetzlar, Germany). Image-Pro Plus 6.0 software was used to compare the fluorescence intensity of FITC-BSA on the membranes.

2.5. In Vitro Biosafety Evaluation

Prepared PCL and PCL-PDA samples with concentrations of 5000, 2500, 1250, 625, 312.5, 156.25 µg/mL and placed in culture medium for 24 hours to make an extract. Cultivated mouse fibroblasts cells (L-929, NCTC) and adjusted density to 1×10^5 /well, inoculated on a 24 well plate. Put 1 mL extraction solution to the pore plate. After 24 hours, added 100 µL CCK-8 reagent. Incubated in a cell culture chamber at 37 °C for 4 hours, and measured the absorbance of the supernatant at 450 nm on an enzyme-linked immunosorbent assay.

Fibrous membranes were sterilized (UV sterilization) for 1 hour, and used PBS solution wash three times to remove residual ethanol. Placed the sample in a 24 well plate and inoculated fibroblasts at a density of 1×10^5 /well on it. On days 1, 3, and 5, cells were stained with Calcein-AM and observed cell growth by laser confocal microscopy (OLYMPUS FV1000, Japan). The third day, removed the culture medium from the well, washed the sample three times with PBS solution, fixed with 3% glutaraldehyde for 12 hours, dehydrated with gradient alcohol, and observed the sample using SEM after gold spraying treatment.

2.6. In Vivo Biosafety Evaluation

To evaluate the biocompatibility and degradability of fiber membranes in vivo, we anesthetized SD rats with pentobarbital sodium and removed hair on the back. After the incision on the back skin, a 20 mg sample was implanted. In the blank group, only skin incision and suture were performed without embedding any material. The positive control group was filter paper. The skin reaction of each group was observed at 0, 3, 7, 14 days. After 14 days, the rats in each group were euthanized, and the whole skin tissue of each group was stained with hematoxylin-eosin (HE) to observe the skin pathological changes (especially foreign body reaction and inflammatory reaction) and evaluate the

degradation performance of the material. In addition, the shape and size of heart, lung, stomach, liver, spleen and kidney of blank group and PCL-PDA group were observed. Then, the pathological changes of these organs were observed by HE staining to assess whether PCL-PDA caused substantial damage to various organs after degradation and absorption.

2.7. Blood Coagulation In Vitro

Fresh rat blood was extracted and mixed with Anticoagulant citrate dextrose solution (ACD, 20mM citric acid, 110mM sodium citrate, 5mM D-glucose) at a ratio of 9:1 (v/v) to make anticoagulant whole blood for later use. The samples of PCL, PCL-PDA and PCL-PD-TB were cut into a square (0.5 x 0.5cm) of the same size and put into the 12-hole plate. The hole plate of the sample was not added as the control group. 50μL anticoagulant whole blood drops were added to the surface of each group of samples, and then 10μL 0.2mol/LCaCl₂ solution was added to initiate coagulation. Then the samples were placed in a constant temperature oscillating incubator at 37°C for 10min, 20min, 30min, 40min, 50min and 60min. After that, 3ml of deionized water was added to each sample, gently shook and left for 5min. Finally, the absorbance of the supernatant was measured at 545nm by enzymograph, and the dynamic coagulation curves of each group were obtained. The whole blood clotting index (BCI) is calculated as follows:

$$BCI = [(A_s - A_b) / (A_c - A_b)] \times 100\% \quad (1)$$

where, A_s is the OD value of the experimental group, A_c is the OD value of the control group, and A_b is the OD value of the blank hole.

Each group of samples was repeated three times.

2.8. Red Blood Cell Adhesion

The PCL, PCL-PDA, and PCL-PDA-TB samples were placed in a 24-well orifice plate. 1mL of anticoagulant whole blood was dropped in each sample. The 24-well plate was incubated in a 37°C incubator for 5min to make the sample fully interact with the blood. Deionized water was then slowly added to the surface of each sample to wash away the red blood cells that had not been captured by the material. After fixation with 3% glutaraldehyde for 12h, dehydration and gold spraying with gradient alcohol were performed. The morphology and number of red blood cells adhering to the surface of the sample were observed by SEM.

2.9. Platelet Adhesion

The procedure of this part of the experiment is similar to that of red blood cell adhesion. The difference was that anticoagulant whole blood was centrifuged at 800rpm for 10min, and the supernatant was obtained with a pipette to obtain platelet-rich plasma (PRP), which was then added to the surface of the sample. Incubate for 2h. Finally, SEM was used to observe the number and activation degree of platelets adhering to the surface of the sample.

2.10. In Vivo Hemostatic Test

All experimental procedures in this study were carried out in accordance with ethical guidelines and approved by the Animal Ethics Committee of Peking University People's Hospital (approval number: 2021PHE067). This part of the experiment used 60 SD rats purchased from Beijing Weitonglihua Laboratory Animal Technology Co., LTD. (License No. SCXK (JING) 2021-0011). Each experimental animal was randomly divided into 5 groups with 6 animals in each group: control group (using ordinary gauze), PCL group, PCL-PDA group, PCL-PD-TB group and commercial group (using absorbable soluble hemostatic material, purchased from Qingdao Zhonghui Shengxi Biological Engineering Co., LTD., Qingdao, China).

Femoral artery hemostasis experiment. The SD rats were anesthetized and fixed in a supine position. The skin and muscle were cut layer by layer from the inner thigh to expose the femoral artery. The femoral artery was punctured with the needle of a 1ml syringe, then materials of each

group were placed at the wound and fully fitted to the wound through appropriate pressure. The time of complete stop of bleeding and the amount of bleeding were recorded.

Liver hemostasis experiment. SD rats were anesthetized, fixed in supine position, shaved, disinfected, and made a median abdominal incision about 5cm long, and cut the skin, muscle and peritoneum layer by layer. The liver was exposed. After the right lobe of the liver was fully exposed, a scalpel was used to make a cutting wound about 0.5cm long and 0.2cm deep on it. The materials of each group were placed in the wound, fully covered and attached to the liver tissue. The dry cotton ball was applied to the wound on the outside of the material. The time of complete stop of blood seepage and the amount of blood loss were recorded.

2.11. Statistical Analysis

All data are expressed as mean \pm standard deviation (SDs). SPSS 13.0 statistical software and one-way analysis of variance (ANOVA) were used to analyze the data. * $P < 0.05$, ** $P < 0.01$, *** $P < 0.001$ were defined as all statistical tests were significant, ns meant $P > 0.05$, and there was no statistical difference in the results.

3. Results

3.1. Characterization of Membranes

The PCL and PCL-PDA nanofiber membranes were observed by SEM. As can be seen from Figure 1A, the distribution of the two scaffolds was uniform and smooth. The surface of PCL fiber membrane was smooth, and the surface of PCL-PDA fiber membrane was rough. The surface elements of PCL and PCL-PDA fiber membranes are also shown in Figure 1A. After PDA coating, the content of N increased from 0 to 3.00%. As can be seen from Figure 1B, the fiber diameter increased from $0.14 \pm 0.05 \mu\text{m}$ to $0.20 \pm 0.11 \mu\text{m}$ after PDA modification. Fiber diameter increased slightly. Figure 1C shows the water contact Angle of PCL and PCL-PDA fiber membranes. After PDA coating, the water contact Angle decreased significantly from $111.47 \pm 1.09^\circ$ to $45.46 \pm 1.27^\circ$ ($P < 0.01$).

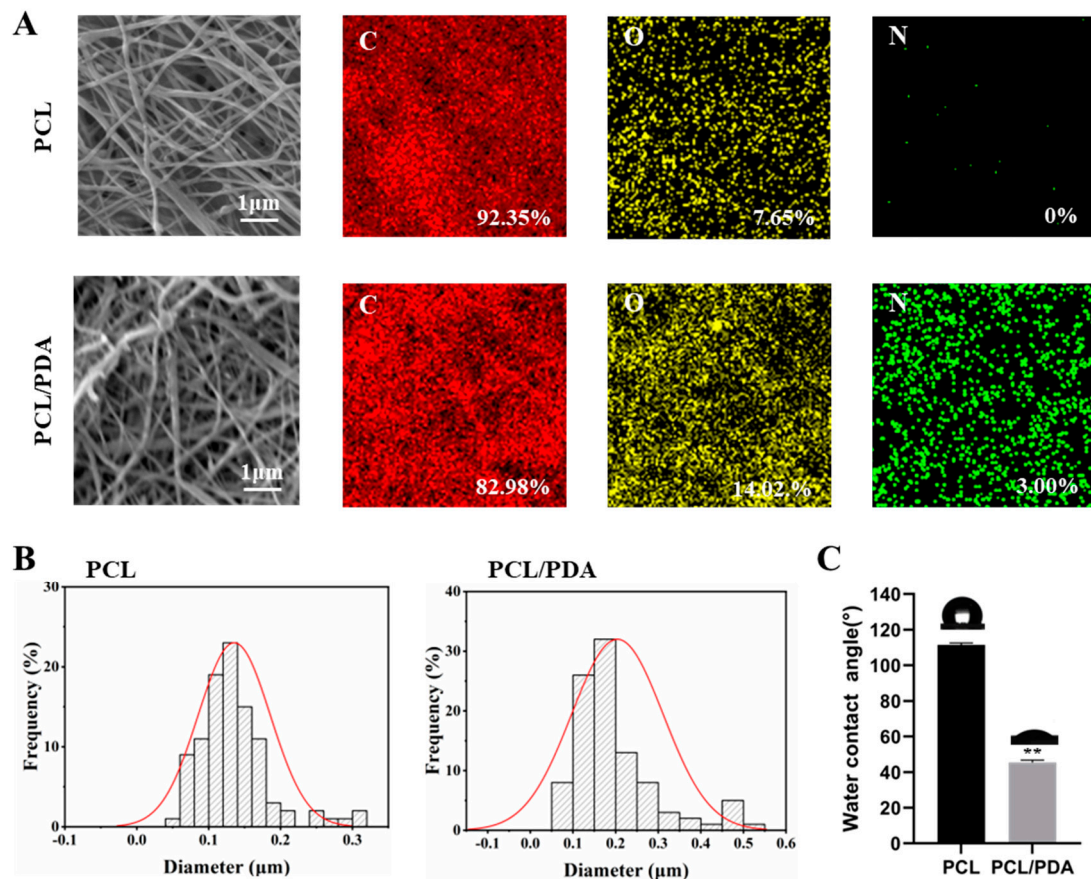


Figure 1. (A) SEM and EDS elemental mapping images of PCL and PCL-PDA fibrous membranes. (B) Fiber diameter distribution of PCL and PCL-PDA fibrous scaffolds. (C) Water contact angles of PCL and PCL-PDA fibrous membranes ($n = 3$, ** $P < 0.01$).

3.2. Loading of Thrombin

Figure 2A shows that the fluorescence intensity of the PCL fiber membrane was much lower than that of the PCL-PDA fiber membrane, indicating that the PCL-PDA fiber membrane was loaded with more thrombin model drug (FITC-BAS). By quantification and comparison of fluorescence intensity (Figure 2B), PCL-PDA fiber membrane was much higher than PCL fiber membrane ($P < 0.01$). We also observed the SEM images and surface element distribution of PCL-TB and PCL-PD-TB fiber membranes loaded with thrombin. As can be seen from Figure S1, the PCL-PDA membrane had more thrombin particles on the fiber surface than the PCL membrane. As shown in Figure S2, the surface of PCL-PD-TB fiber membrane has increased the S element specific to thrombin. The results showed that thrombin was loaded onto the surface of PCL-PDA fiber membrane.

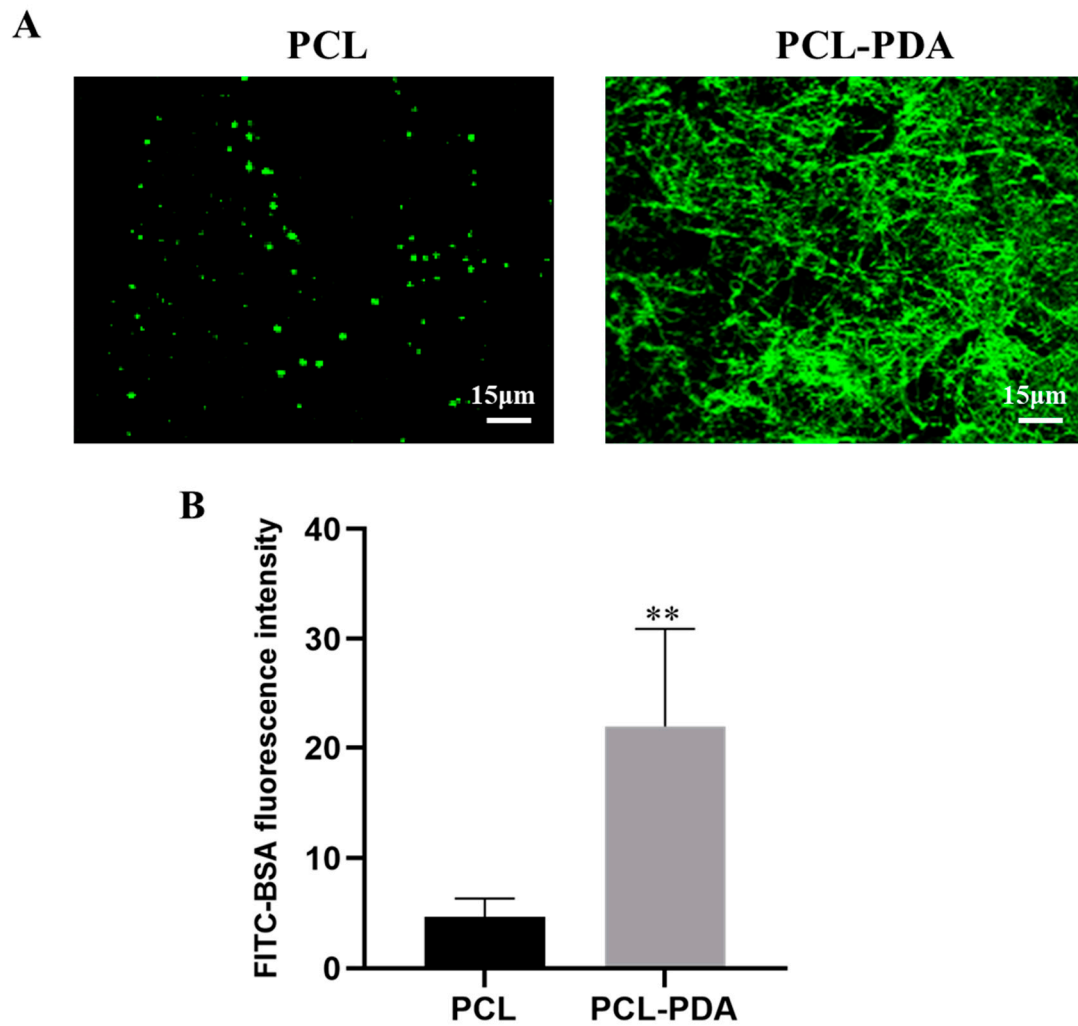


Figure 2. (A) CLSM images of FITC-BSA loaded onto PCL and PCL-PDA fibrous membranes. (B) Fluorescence intensity of FITC-BAS on PCL and PCL-PDA fibrous membranes (n = 6, ** P < 0.01).

3.3. *In Vitro Safety Evaluation of Membranes*

The detection results of CCK8 are shown in Figure 3A. The survival rate of membranes cultured with different concentrations of PCL and PCL-PDA fiber membranes was more than 90% after 1 day, indicating that both membranes had good biocompatibility. As shown in Figure 3B, in the SEM images after 3 days of culture, more membranes were adhered to the PCL-PDA fiber membrane than the PCL fiber membrane. On days 1, 3, and 5, living cells were colored green by Calcein-AM and dead cells were colored red by PI. There was little red fluorescence in Figure 3C. The results also showed that PCL fiber membrane and PCL-PDA fiber membrane had good cytocompatibility.

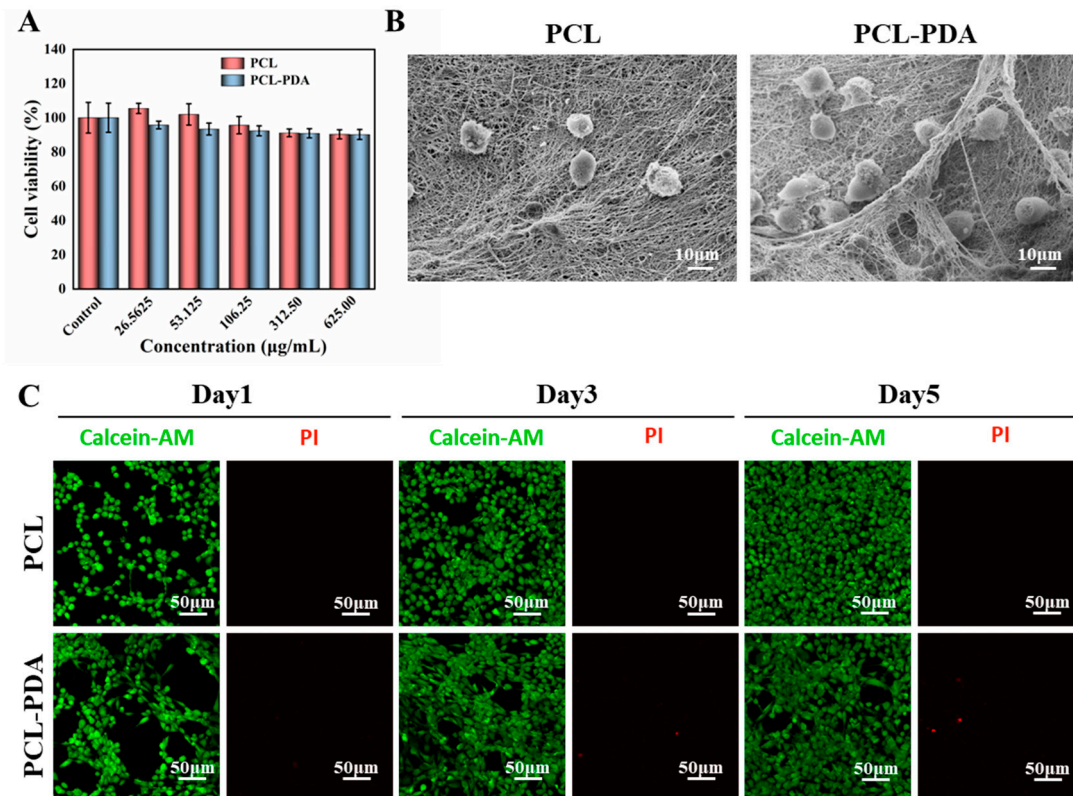


Figure 3. (A) Cell viability of PCL and PCL-PDA fibrous membranes incubated with Fibroblasts cells for 1 day. (B) SEM images of Fibroblasts cells grown on PCL and PCL-PDA fibrous membranes. (C) Representative CLSM images of fibroblasts cells after 1day, 3 days and 5 days of culture on PCL and PCL-PDA fibrous membranes.

3.4. In Vivo Biosafety Assessment of Membranes

To further evaluate the biosafety of the membranes, filter paper (control group), PCL, and PCL-PDA fiber membranes were implanted into the subcutaneous tissue of the rat back (Figure 4A). The images of the wound were recorded after the operation. On the 7th day, the wounds of the control group showed obvious redness and swelling. After 14 days, all wounds recovered completely. HE results showed that the control group had relatively serious foreign body granuloma and inflammatory reaction, while the cells in other groups maintained normal levels, indicating that PCL and PCL-PDA fiber membranes had good biosafety and degradation performance.

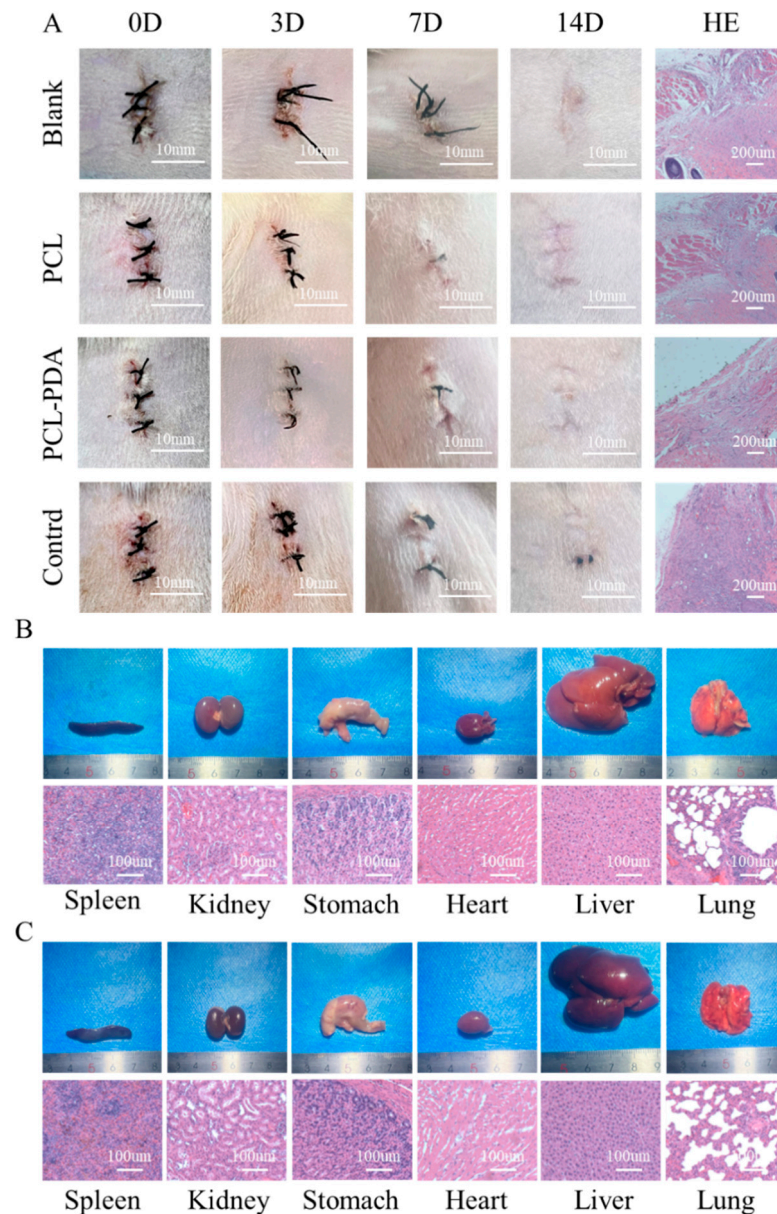


Figure 4. (A) Photographs of the wounds that were embedded the PCL, PCL-PDA, control group and blank group samples immediately following surgery (day 0), and for 3, 7, 14 day. Histological analysis of subcutaneous tissue of the wounds after embedding surgery at 14 days. Photographs and histological analysis for rat internal organs (heart, lung, stomach, liver, spleen and kidney) after 14 days embedding experiment with PCL-PDA (B) and blank group (C), respectively.

In order to further investigate the biotoxic effects of PCL-PDA fiber membranes and their degradation products on other organs, including heart, lung, stomach, liver, spleen and kidney, we compared the gross and HE results of various organs in SD rats after 14 days of subcutaneous implantation of PCL-PDA fiber membranes. As shown in Figure 4B,C, the shape and size of each organ in the PCL-PDA group did not change significantly, which was similar to that of normal rats. After histological analysis, no substantial damage was found in the organs of the rats treated with PCL-PDA, indicating that there were no obvious side effects on the circulatory system, respiratory system, digestive system and metabolic system.

3.5. Evaluation of *In Vitro* Blood Clotting of Membranes

We evaluated the blood coagulability of membranes *in vitro*. Blood after adding calcium ions was dripped onto the surface of the membrane, and sample photos and BIC were recorded at different

time points to measure the coagulation ability of membranes. As shown in Figure 5A, at 10min, the supernatant clarity of PCL-PDA-TB fiber membrane was significantly higher than that of the control group, PCL and PCL-PDA groups. This result corresponded to the BCI index result. At 10min, the BCI of PCL-PDA-TB fiber membrane ($20.29 \pm 4.05\%$) was significantly lower than that of PCL fiber membrane ($114.83 \pm 18.53\%$, $P < 0.001$) and PCL-PDA fiber membrane ($94.96 \pm 11.33\%$, $P < 0.01$). During the whole experiment, the BCI of PCL-PDA-TB membrane was lower than that of PCL and PCL-PDA membrane, indicating that the coagulability and efficiency of PCL-PDA-TB membrane were significantly improved after thrombin loading.

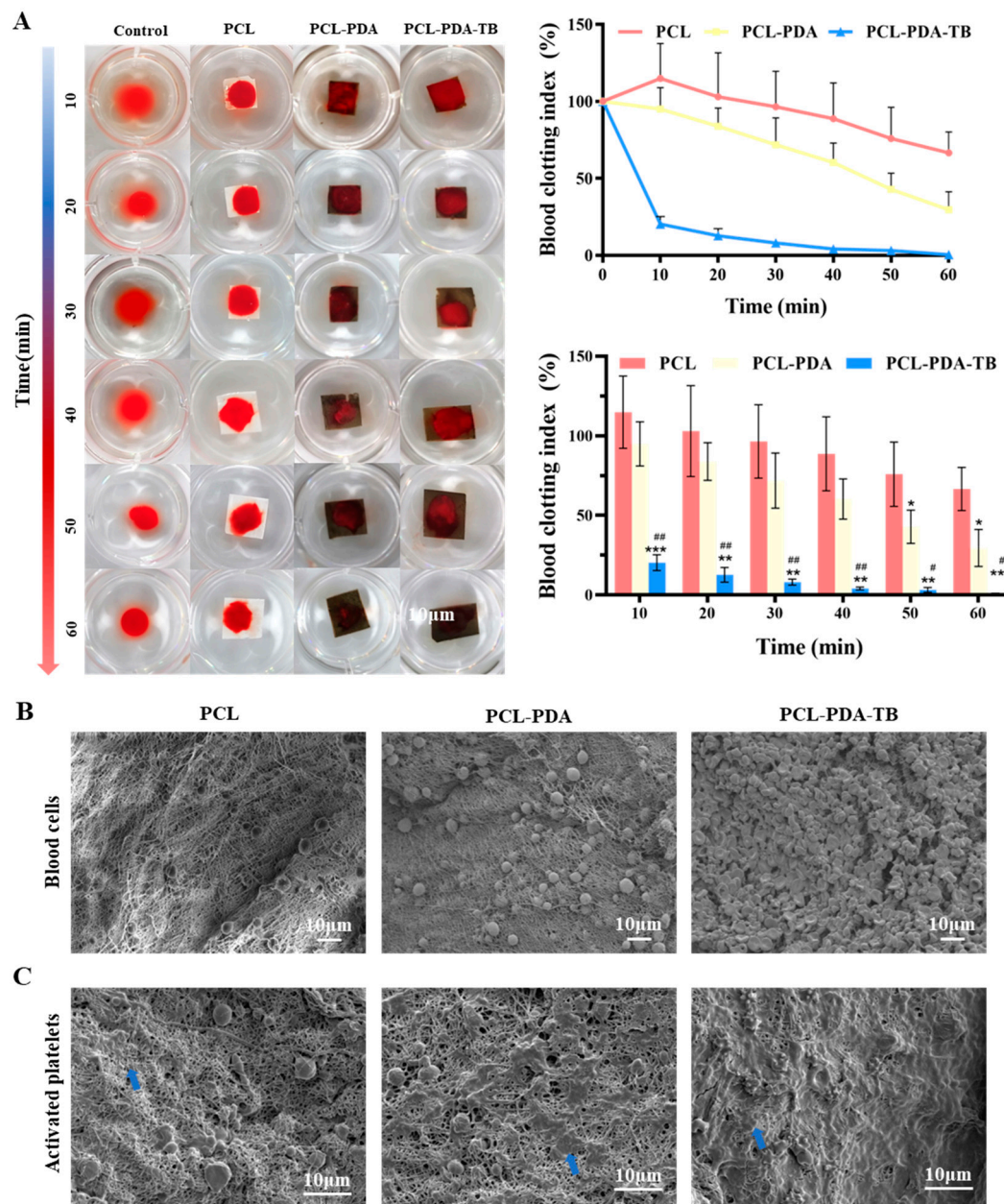


Figure 5. (A) Photographs from the in vitro blood-clotting measurement and the Blood clotting index of the supernatant absorbance for PCL, PCL-PDA, PCL-PDA-TB ($n = 3$, ** $P < 0.01$, versus PCL group; *** $P < 0.001$, versus PCL group; # $P < 0.05$, versus PCL-PDA group; ## $P < 0.01$, versus PCL-PDA group). The SEM images of blood cells (B) and activated platelets (C) on the PCL, PCL-PDA, PCL-PDA-TB surface (blue arrow).

Further, we evaluated the coagulation properties of PCL, PCL-PDA, and PCL-PD-TB membranes at the microscopic level by SEM images of red blood cell adhesion to platelets. Thrombin

can perform hemostasis by converting fibrinogen to fibrin and activating clotting factor XIII to obtain stable fibrin clots. In addition, thrombin activates proteinase-activating receptors on the surface of platelets, causing platelets to activate and promoting platelet adhesion. This is because thrombin on the scaffold causes stable fibrin grids to form quickly in the blood to trap and adsorb more blood material. It can be seen from Figure 5C that compared with PCL and PCL-PDA fiber membranes, there was more activated platelet adhesion on the surface of PCL-PD-TB. These results indicated that PCL-PDA fiber membranes can maintain thrombin activity and exert coagulation ability after thrombin loading.

3.6. Evaluation of Hemostatic Performance In Vivo

We first tested the hemostatic performance of PCL, PCL-PDA, and PCL-PD-TB membranes in the femoral artery bleeding model of SD rats (Figure 6A). As can be seen from Figure 6B,C, the amount of blood loss (198.33 ± 2.91 mg) and bleeding time (45.00 ± 1.69 s) in the PCL-PDA-TB group were significantly lower than those in the control group (1099.67 ± 3.14 mg, 106.83 ± 6.43 s, $P < 0.001$), PCL group (775.50 ± 5.41 mg, 66.50 ± 1.50 s, $P < 0.001$) and PCL-PDA group (444.00 ± 13.47 mg, 50.33 ± 1.50 s, $P < 0.001$). There was no significant difference in blood loss and bleeding time between the PCL-PDA-TB group and the commercial group (186.00 ± 4.55 mg, 39.50 ± 0.96 s, $P > 0.05$).

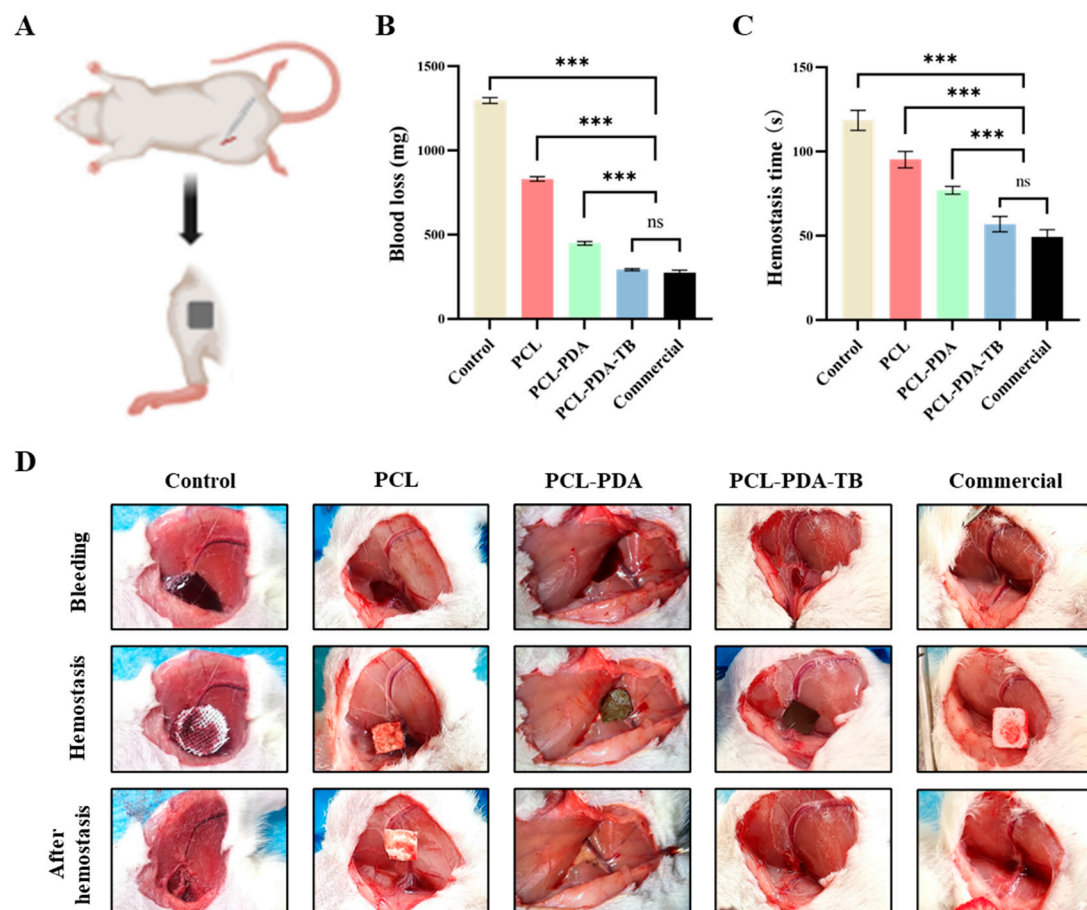


Figure 6. (A) Schematic diagram of the rat femoral artery haemostasis model. (B) Blood loss and (C) hemostatic time on the rat femoral artery haemostasis model by using control, PCL, PCL-PDA, PCL-PDA-TB and commercial. (D) Images of the hemostasis (from left to right) by use of control, PCL, PCL-PDA, PCL-PDA-TB and commercial ($n = 6$, *** $P < 0.001$).

Then, we tested the hemostatic performance of PCL, PCL-PDA, and PCL-PD-TB membranes in a liver dissection model of SD rats (Figure 7A). We found that the amount of blood loss (292.35 ± 5.75 mg) and bleeding time (56.83 ± 4.49 s) in the PCL-PDA-TB group were significantly lower than those

in the control group (1296.51 ± 15.28 mg, 118.50 ± 5.44 s, $P < 0.001$), PCL group (831.77 ± 11.67 mg, 95.17 ± 4.49 s, $P < 0.001$) and PCL-PDA group (449.33 ± 9.73 mg, 77.00 ± 2.16 s, $P < 0.001$). There was no significant difference in blood loss volume and bleeding time between the PCL-PDA-TB group and the commercial group (275.34 ± 12.75 mg, 49.33 ± 3.86 s, $P > 0.05$) (Figure 7B,C). The above results indicate that PCL-PDA-TB has good hemostatic performance in vivo, which is close to that of commercial dressings.

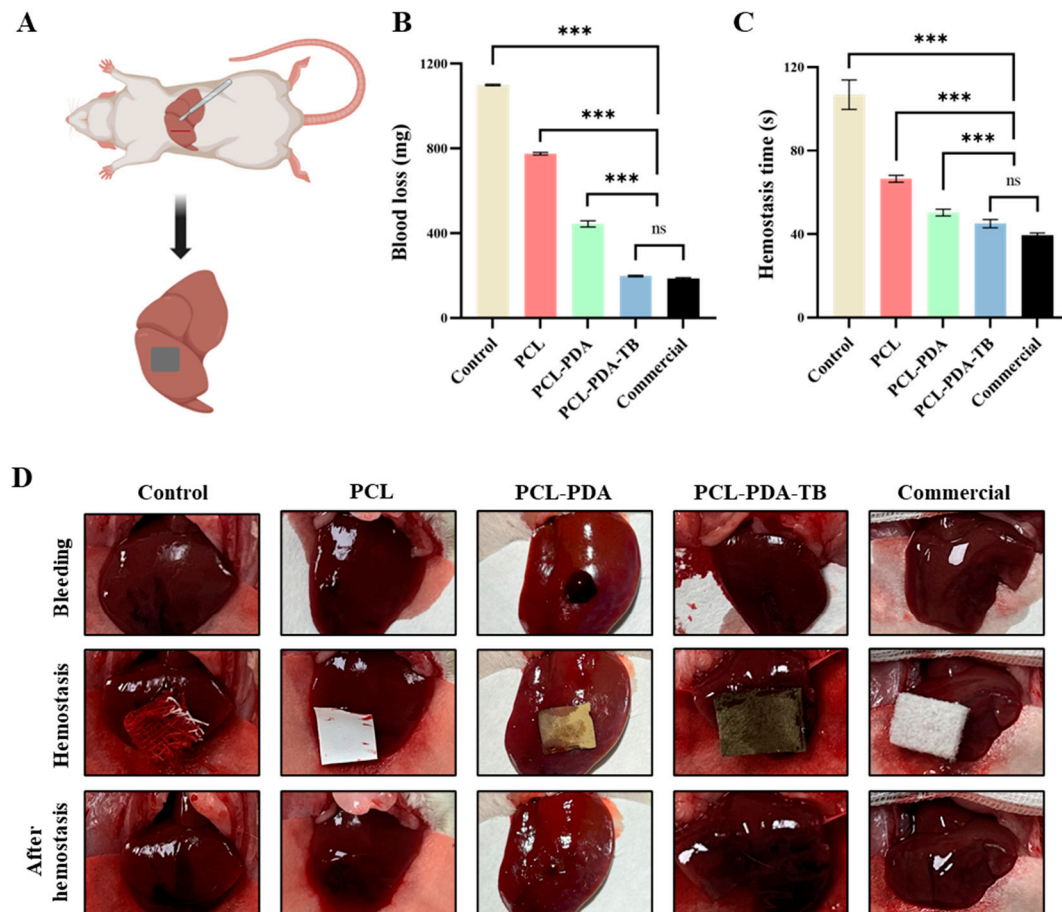


Figure 7. (A) Schematic diagram of the rat liver haemostasis model. (B) Blood loss and (C) hemostatic time on the rat liver haemostasis model by using control, PCL, PCL-PDA, PCL-PDA-TB and commercial. (D) Images of the hemostasis (from left to right) by use of control, PCL, PCL-PDA, PCL-PDA-TB and commercial ($n = 6$, *** $P < 0.001$).

4. Discussion

The ideal hemostatic material should have the following characteristics: rapid, clear hemostatic effect; easy to make, portable and use; safe and non-toxic, good biocompatibility; multiple bleeding scenarios [29,30]. Due to the complexity and coordination of coagulation mechanisms, no hemostatic material has been able to fully meet the above hemostatic criteria so far. Therefore, exploring and developing new rapid hemostatic materials with better performance and hemostatic effect is still an urgent need for trauma first aid.

Thrombin is a coagulation system protease excited by sodium ions that plays a key role in the coagulation cascade [31]. After a traumatic event, thrombin rapidly converts from inactive prothrombin to thrombin and immediately participates in coagulation and hemostasis [32]. However, numerous previous studies have found that the thrombin produced by autoprothrombin is far from sufficient to meet the needs of local or systemic trauma hemostasis in response to more severe traumatic bleeding. Some studies have tried to incorporate thrombin into hemostatic materials, but failed to solve outstanding problems such as low thrombin load and poor storage conditions [33,34].

PDA can simulate the mucous components secreted by Marine mussel byssus from the perspective of bionics, and bind to the surface of inorganic, organic, metal, polymer and other substrates [35]. The PDA bound to the surface of the material has the ability to adsorb a large number of active proteins [36]. In this study, a new hemostatic dressing with good hemostatic performance and easy storage at room temperature was prepared by using electrostatic spinning nanofiber membrane modified by PDA to increase thrombin load and stability under the premise of ensuring biological activity. In vitro experiments, the good microstructure, high thrombin load and biocompatibility of the new hemostatic material were effectively verified by SEM, CLMS, cell proliferation experiment, cell adhesion experiment and extract cytotoxicity experiment. Erythrocyte adhesion, platelet adhesion, dynamic coagulation time and animal model experiments proved the good coagulation effect of thrombin nanofiber membrane.

Electrospinning is a common method for preparing hemostatic materials [37,38]. Electrospinning technology mainly includes four parts: high voltage, propel pump, syringe and receiving device [39]. Nanofibers prepared by electrospinning technology have high porosity, gas permeability, and can provide a high specific surface area [40], which are conducive to removing exudate and achieving hemostasis. Commonly used polymers for hemostatic materials include PEO, PLA, PCL, PVA, etc., which often have high mechanical properties, but worse biocompatibility than natural materials [41,42]. In fact, in the actual hemostatic scene, it is difficult to achieve efficient hemostasis by relying only on the physical properties and morphological characteristics of the nanofibers, so adding additional drugs with excellent hemostatic performance is a potential solution. In order to overcome the hydrophobic characteristics of pure polymer electrospinning membrane, we used PDA surface modification to load thrombin onto PCL fiber membrane. Through SEM image and surface chemical element analysis, it was found that PDA was successfully coated on the PCL fiber membrane surface without damaging the microstructure of the membrane. The results of water contact showed that the surface hydrophilicity of PCL fiber membrane increased significantly after PDA coating. Studies have shown that hydrophilic surfaces are more conducive to cell adhesion and proliferation [43]. In addition, CLMS observation and SEM image results showed that the thrombin load on PCL fiber membrane increased significantly after PDA coating. These results indicate that the thrombin loading system based on the PDA surface modification has been successfully developed.

Thrombin can convert fibrinogen to fibrin and activate platelets, causing platelet aggregation to promote clotting or hemostasis [44]. In the test of blood coagulation in vitro, we found that PCL-PDA fiber membrane loaded with thrombin can rapidly promote blood coagulation. These results indicate that thrombin can still exert normal coagulation function in PCL-PDA loading system, promote the formation of fibrin mesh and platelet adhesion, and form stable thrombus. On the basis of the positive results in vitro, the effect of these membranes on hemostasis in vivo was further evaluated. The PADD-modified PCL fiber membrane is used to connect thrombin to form thrombin membrane, which overcomes the shortcomings of thrombin powder, such as poor strength, easy to fall off and unstable hemostatic effect caused by premature autolysis [45]. In the experimental model of femoral artery bleeding and liver bleeding in SD rats, PCL-PD-TB fiber membrane can quickly infiltrate and absorb blood, and maintain a stable shape during hemostasis, so that thrombin can continue to play the hemostatic function. The above properties make the hemostatic performance of PCL-PD-TB significantly better than the other two membranes, and there is no significant difference with commercial hemostatic dressing.

However, this study also has some shortcomings that need to be further improved in the future, mainly including: (1) limited by research conditions, we have not been able to explore the related repair mechanism of hemostasis, which caused the lack of theoretical support and hemostatic repair mechanism could be an important research direction in the future; (2) The traumatic bleeding models in this study were New Zealand white rabbits and SD rats, we did not use larger animals such as Bama pigs for further hemostasis verification studies. The application of more advanced traumatic bleeding models and human trials are important research directions for research on hemostatic materials; (3) the small number of animal samples in this study may cause certain bias in the study,

and multi-angle multiple hemostatic effect verification will be carried out to further confirm the hemostatic effect of the hemostatic material.

5. Conclusion

In this study, PCL-PD-TB fibrous scaffolds were prepared and their hemostatic performance was evaluated using in vitro and in vivo models. In vitro, the PCL-PDA-TB fiber scaffold can maintain the stable load and biological activity of thrombin, and significantly promoted red blood cell adhesion and activation. In vivo, the PCL-PDA-TB fiber stent showed similar effects to commercial hemostatic dressings. The effect of the PCL-PDA-TB fiber scaffold was believed to be the result of a combination of favorable factors, including the electrospun nanofibers, the surface modification of the PDA, and the continuous action of thrombin. In conclusion, PCL-PDA-TB fiber stent can be considered as a hemostatic dressing with clinical application potential.

Author Contributions: Conceptualization, M.L., W.G. and T.W.; Methodology, D.C. and P.Z.; Software, F.R.; Validation, W.H., P.Z. and F.R.; Investigation, W.H.; Resources, T.W.; Data Curation, C.W.; Writing – Original Draft Preparation, D.C. and M.L.; Writing – Review & Editing, T.W. and W.G.; Visualization, D.C. and P.Z.; Supervision, T.W.; Project Administration, W.G. and C.W.; Funding Acquisition, T.W. and W.G.

Funding: This study was funded by grants from Beijing Natural Science Foundation (7232185), Natural Science Foundation of China (31801009, 81901251), Health Innovation Special Project of Hebei Provincial Key R&D Program (223777101D) and Peking University People's Hospital Scientific Research Development Funds (RDG2021-06).

Institutional Review Board Statement: The study was conducted according to the guidelines of the Declaration of Helsinki, and approved by the Animal Ethics Committee of Peking University People's Hospital (approval number: 2021PHE067).

Data Availability Statement: All data that support the findings of this study are included within the article (and any supplementary files).

Acknowledgments: We gratefully acknowledge Dr Tiantian Min for their assistance in preparing the electrospun nanofiber membranes and providing technical support. We also thank Dr Wei Pi for technical assistance.

Conflicts of Interest: There are no conflicts of interest.

Reference

1. Champion HR, Bellamy RF, Roberts CP, Leppaniemi A. A profile of combat injury. *J Trauma*. 2003 May;54(5 Suppl):S13-9.
2. Stewart RM, Myers JG, Dent DL, Ermis P, Gray GA, Villarreal R, Blow O, Woods B, McFarland M, Garavaglia J, Root HD, Pruitt BA Jr. Seven hundred fifty-three consecutive deaths in a level I trauma center: the argument for injury prevention. *J Trauma*. 2003 Jan;54(1):66-70; discussion 70-1.
3. Kauvar DS, Lefering R, Wade CE. Impact of hemorrhage on trauma outcome: an overview of epidemiology, clinical presentations, and therapeutic considerations. *J Trauma*. 2006 Jun;60(6 Suppl):S3-11.
4. Muldowney M, Liu Z, Stansbury LG, Vavilala MS, Hess JR. Ultramassive Transfusion for Trauma in the Age of Hemostatic Resuscitation: A Retrospective Single-Center Cohort From a Large US Level-1 Trauma Center, 2011-2021. *Anesth Analg*. 2023 May 1;136(5):927-933.
5. Sperry JL, Cotton BA, Luther JF, Cannon JW, Schreiber MA, Moore EE, Namias N, Minei JP, Wisniewski SR, Guyette FX; Shock Whole blood and Assessment of Traumatic brain injury (SWAT) study group. Whole Blood Resuscitation and Association with Survival in Injured Patients with an Elevated Probability of Mortality. *J Am Coll Surg*. 2023 Apr 11.
6. Wang Y, Wang C, Hu P, Wang H, Gan L, Kong G, Shi Y, Wang T, Jiang B. China trauma treatment statistics 2019: A national retrospective study based on hospitalized cases. *Front Public Health*. 2023 Feb 24;11:1116828.

7. Wang T, Wang Y, Xu T, Li L, Huo M, Li X, He Y, Lin Q, Mei B, Zhou X, Jiang B. Epidemiological and clinical characteristics of 3327 cases of traffic trauma deaths in Beijing from 2008 to 2017: a retrospective analysis. *Medicine (Baltimore)*. 2020 Jan;99(1):e18567.
8. Gu H, Li H, Wei L, Lu J, Wei Q. Collagen-based injectable and self-healing hydrogel with multifunction for regenerative repairment of infected wounds. *Regen Biomater*. 2023 Mar 7;10:rbad018.
9. Ibne Mahbub MS, Bae SH, Gwon JG, Lee BT. Decellularized liver extracellular matrix and thrombin loaded biodegradable TOCN/Chitosan nanocomposite for hemostasis and wound healing in rat liver hemorrhage model. *Int J Biol Macromol*. 2023 Jan 15;225:1529-1542.
10. Das P, Manna S, Roy S, Nandi SK, Basak P. Polymeric biomaterials-based tissue engineering for wound healing: a systemic review. *Burns Trauma*. 2023 Feb 7;11:tkac058.
11. Lu X, Li X, Yu J, Ding B. Nanofibrous hemostatic materials: Structural design, fabrication methods, and hemostatic mechanisms. *Acta Biomater*. 2022 Dec;154:49-62.
12. Mecwan M, Li J, Falcone N, Ermis M, Torres E, Morales R, Hassani A, Haghniaz R, Mandal K, Sharma S, Maity S, Zehtabi F, Zamanian B, Herculano R, Akbari M, V John J, Khademhosseini A. Recent advances in biopolymer-based hemostatic materials. *Regen Biomater*. 2022 Sep 21;9:rbac063.
13. Mogoşanu GD, Grumezescu AM. Natural and synthetic polymers for wounds and burns dressing. *Int J Pharm*. 2014 Mar 25;463(2):127-36.
14. Xiao X, Wu Z. A Narrative Review of Different Hemostatic Materials in Emergency Treatment of Trauma. *Emerg Med Int*. 2022 Oct 21;2022:6023261.
15. Zou CY, Li QJ, Hu JJ, Song YT, Zhang QY, Nie R, Li-Ling J, Xie HQ. Design of biopolymer-based hemostatic material: Starting from molecular structures and forms. *Mater Today Bio*. 2022 Oct 18;17:100468.
16. Valke LLFG, Rijpma S, Meijer D, Schols SEM, van Heerde WL. Thrombin generation assays to personalize treatment in bleeding and thrombotic diseases. *Front Cardiovasc Med*. 2022 Nov 10;9:1033416.
17. Al-Amer OM. The role of thrombin in haemostasis. *Blood Coagul Fibrinolysis*. 2022 Apr 1;33(3):145-148.
18. Jiang SX, Chahal D, Ali-Mohamad N, Kastrup C, Donnellan F. Hemostatic powders for gastrointestinal bleeding: a review of old, new, and emerging agents in a rapidly advancing field. *Endosc Int Open*. 2022 Aug 15;10(8):E1136-E1146.
19. Sidonio RF Jr, Hoffman M, Kenet G, Dargaud Y. Thrombin generation and implications for hemophilia therapies: A narrative review. *Res Pract Thromb Haemost*. 2022 Dec 21;7(1):100018.
20. Shaw JR, Castellucci LA, Siegal D, Carrier M. DOAC-associated bleeding, hemostatic strategies, and thrombin generation assays - a review of the literature. *J Thromb Haemost*. 2023 Mar;21(3):433-452.
21. Hong J, Yeo M, Yang GH, Kim G. Cell-Electrospinning and Its Application for Tissue Engineering. *Int J Mol Sci*. 2019 Dec 9;20(24):6208. doi: 10.3390/ijms20246208. PMID: 31835356; PMCID: PMC6940787.
22. Chamundeswari VN, Yuan Siang L, Jin Chuah Y, Shi Tan J, Wang DA, Loo SCJ. Sustained releasing sponge-like 3D scaffolds for bone tissue engineering applications. *Biomed Mater*. 2017 Dec 28;13(1):015019. doi: 10.1088/1748-605X/aa8bcd. PMID: 28895559.
23. Siddiqui N, Asawa S, Birru B, Baadhe R, Rao S. PCL-Based Composite Scaffold Matrices for Tissue Engineering Applications. *Mol Biotechnol*. 2018 Jul;60(7):506-532. doi: 10.1007/s12033-018-0084-5. PMID: 29761314.
24. Song L, Ahmed MF, Li Y, Bejoy J, Zeng C, Li Y. PCL-PDMS-PCL Copolymer-Based Microspheres Mediate Cardiovascular Differentiation from Embryonic Stem Cells. *Tissue Eng Part C Methods*. 2017 Oct;23(10):627-640. doi: 10.1089/ten.TEC.2017.0307. Epub 2017 Sep 28. PMID: 28826352.
25. Grossen P, Witzigmann D, Sieber S, Huwyler J. PEG-PCL-based nanomedicines: A biodegradable drug delivery system and its application. *J Control Release*. 2017 Aug 28;260:46-60. doi: 10.1016/j.jconrel.2017.05.028. Epub 2017 May 20. PMID: 28536049.

26. Zhou S, Chang Q, Lu F, Xing M. Injectable Mussel-Inspired Immobilization of Platelet-Rich Plasma on Microspheres Bridging Adipose Micro-Tissues to Improve Autologous Fat Transplantation by Controlling Release of PDGF and VEGF, Angiogenesis, Stem Cell Migration. *Adv Healthc Mater.* 2017 Nov;6(22). doi: 10.1002/adhm.201700131. Epub 2017 Sep 7. PMID: 28881440.
27. Lee SJ, Kim ME, Nah H, Seok JM, Jeong MH, Park K, Kwon IK, Lee JS, Park SA. Vascular endothelial growth factor immobilized on mussel-inspired three-dimensional bilayered scaffold for artificial vascular graft application: In vitro and in vivo evaluations. *J Colloid Interface Sci.* 2019 Mar 1;537:333-344. doi: 10.1016/j.jcis.2018.11.039. Epub 2018 Nov 12. PMID: 30453227.
28. Pi W, Zhang Y, Li L, Li C, Zhang M, Zhang W, Cai Q, Zhang P. Polydopamine-coated polycaprolactone/carbon nanotube fibrous scaffolds loaded with brain-derived neurotrophic factor for peripheral nerve regeneration. *Biofabrication.* 2022 Apr 20;14(3). doi: 10.1088/1758-5090/ac57a6. PMID: 35193120.
29. Muzzarelli R. Chitins and chitosans for the repair of wounded skin, nerve, cartilage and bone[J]. *Carbohydrate Polymers*, 2009, 76(2):167-182.
30. Pendharkar S, Jian G. Biodegradable hemostatic wound dressings: US, US20040241212 A1[P]. 2004.
31. Mısırlıoğlu S, Türkgeldi E, Yağmur H, Urman B, Ata B. Use of a gelatin-thrombin hemostatic matrix in obstetrics and gynecological surgery. *Turk J Obstet Gynecol.* 2018 Sep;15(3):193-199.
32. Wasilko SM, Quinlan NJ, Shafritz AB. Topical hemostatic agents and their role in upper extremity surgery. *J Hand Surg Am.* 2015 Mar;40(3):602-4.
33. Lawson JH. The clinical use and immunologic impact of thrombin in surgery. *Semin Thromb Hemost.* 2006 Apr;32 Suppl 1:98-110.
34. Takeda K. [Role of increase in permeability and circulatory failure in the development of organ dysfunction in severe acute pancreatitis]. *Nihon Rinsho.* 2004 Nov;62(11):1999-2004.
35. Zhao H, Waite JH. Linking adhesive and structural proteins in the attachment plaque of *Mytilus californianus*. *J Biol Chem.* 2006 Sep 8;281(36):26150-8. doi: 10.1074/jbc.M604357200. Epub 2006 Jul 14. PMID: 16844688.
36. Liu Y, Ai K, Lu L. Polydopamine and its derivative materials: synthesis and promising applications in energy, environmental, and biomedical fields. *Chem Rev.* 2014 May 14;114(9):5057-115. doi: 10.1021/cr400407a. Epub 2014 Feb 11. PMID: 24517847.
37. Sánchez-Machado DI, Maldonado-Cabrera A, López-Cervantes J, Maldonado-Cabrera B, Chávez-Almanza AF. Therapeutic effects of electrospun chitosan nanofibers on animal skin wounds: A systematic review and meta-analysis. *Int J Pharm X.* 2023 Mar 1;5:100175.
38. Pilehvar-Soltanahmadi Y, Dadashpour M, Mohajeri A, Fattahi A, Sheervalilou R, Zarghami N. An Overview on Application of Natural Substances Incorporated with Electrospun Nanofibrous Scaffolds to Development of Innovative Wound Dressings. *Mini Rev Med Chem.* 2018 Feb 14;18(5):414-427.
39. Xue J, Wu T, Dai Y, Xia Y. Electrospinning and Electrospun Nanofibers: Methods, Materials, and Applications. *Chem Rev.* 2019 Apr 24;119(8):5298-5415.
40. Elangwe CN, Morozkina SN, Olekhovich RO, Polyakova VO, Krasichkov A, Yablonskiy PK, Uspenskaya MV. Pullulan-Based Hydrogels in Wound Healing and Skin Tissue Engineering Applications: A Review. *Int J Mol Sci.* 2023 Mar 4;24(5):4962.
41. Petroni S, Tagliaro I, Antonini C, D'Arienzo M, Orsini SF, Mano JF, Brancato V, Borges J, Cipolla L. Chitosan-Based Biomaterials: Insights into Chemistry, Properties, Devices, and Their Biomedical Applications. *Mar Drugs.* 2023 Feb 24;21(3):147.
42. Erdi M, Sandler A, Kofinas P. Polymer nanomaterials for use as adjuvant surgical tools. *Wiley Interdiscip Rev Nanomed Nanobiotechnol.* 2023 Apr 12:e1889.
43. Wu R, Gao G, Xu Y. Electrospun Fibers Immobilized with BMP-2 Mediated by Polydopamine Combined with Autogenous Tendon to Repair Developmental Dysplasia of the Hip in a Porcine Model. *Int J Nanomedicine.* 2020 Sep 7;15:6563-6577. doi: 10.2147/IJN.S259028. PMID: 32982218; PMCID: PMC7490068.

44. Dimitroulis D, Antoniou E, Karidis NP, Kontzoglou K, Kouraklis G. Surgical control of life-threatening post-ERCP bleeding with a gelatin matrix-thrombin hemostatic agent. *Int J Surg Case Rep.* 2012;3(9):471-3. doi: 10.1016/j.ijscr.2012.05.014. Epub 2012 Jun 2. PMID: 22743012; PMCID: PMC3397303.
45. Coughlin SR. Protease-activated receptors and platelet function. *Thromb Haemost.* 1999 Aug;82(2):353-6. PMID: 10605724.

Disclaimer/Publisher's Note: The statements, opinions and data contained in all publications are solely those of the individual author(s) and contributor(s) and not of MDPI and/or the editor(s). MDPI and/or the editor(s) disclaim responsibility for any injury to people or property resulting from any ideas, methods, instructions or products referred to in the content.